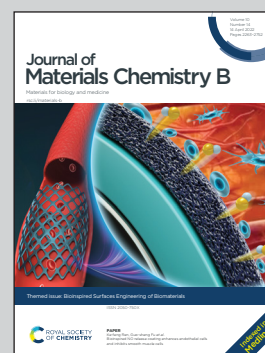**Showcasing research from the Zheng Lab at The University of Akron, USA**

Fundamentals and exploration of aggregation-induced emission molecules for amyloid protein aggregation

AIE molecules enable detection of different amyloid protein aggregates in human tissues associated with different neurodegenerative diseases.

ROYAL SOCIETY
OF **CHEMISTRY**

rsc.li/materials-b

REVIEW

Fundamentals and exploration of aggregation-induced emission molecules for amyloid protein aggregation

Yijing Tang, Dong Zhang, [ID] Yanxian Zhang, Yonglan Liu, [ID] Lirong Cai, Eleanor Plaster and Jie Zheng [ID] *

The past decade has witnessed the growing interest and advances in aggregation-induced emission (AIE) molecules as driven by their unique fluorescence/optical properties in particular sensing applications including biomolecule sensing/detection, environmental/health monitoring, cell imaging/tracking, and disease analysis/ diagnosis. In sharp contrast to conventional aggregation-caused quenching (ACQ) fluorophores, AIE molecules possess intrinsic advantages for the study of disease-related protein aggregates, but such studies are still at an infant stage with much less scientific exploration. This outlook mainly aims to provide the first systematic summary of AIE-based molecules for amyloid protein aggregates associated with neurodegenerative diseases. Despite a limited number of studies on AIE−amyloid systems, we will survey recent and important developments of AIE molecules for different amyloid protein aggregates of Aβ (associated with Alzheimer's disease), insulin (associated with type 2 diabetes), (α-syn, associated with Parkinson's disease), and HEWL (associated with familial lysozyme systemic amyloidosis) with a particular focus on the working principle and structural design of four types of AIE-based molecules. Finally, we will provide our views on current challenges and future directions in this emerging area. Our goal is to inspire more researchers and investment in this emerging but less explored subject, so as to advance our fundamental understanding and practical design/usages of AIE molecules for disease-related protein aggregates.

1. Introduction

Aggregation-induced emission (AIE) molecules have emerged as a new class of materials for their promising applications in environmental/health monitoring, disease diagnosis, bioactive molecule detectors, and electronic devices, due to their excellent sensitivity, rapid response, and inverse fluorescence emission/ quenching effect.[1] In sharp contrast to conventional aggregation-caused quenching (ACQ) fluorophores that always suffer from severe self-quenching, poor photostability, and small Stokes shift in the aggregated state, AIE molecules, as discovered in 2001,[2] emit strong fluorescence in the aggregated state, but weak or no fluorescence in the isolated state, which greatly expands their usage for different sensing applications. The past two decades have witnessed the growing interest and advances of different AIE molecules with different AIE mechanisms (Fig. 1), including (i) tetraphenylethene (TPE), tetraphenylbutadiene (TPBD), quinoline-malononitrile (QM), and hexaphenylsilole (HPS) as designed by restriction of intramolecular motion (RIM),[3,4]

Department of Chemical, Biomolecular, and Corrosion Engineering,
The University of Akron, Ohio, USA. E-mail: zhengj@uakron.edu

(ii) N-(4-(benzo[*d*]thiazol-2-yl)-3-hydroxyphenyl)benzamide (BTHPB), benzothiazole-rhodol derivatives (Rh-F), and myricetin by excited state intramolecular proton transfer (ESIPT),[5–7] (iii) 9,10-bis(*p*-dialkylaminostyryl)anthracene derivatives (9,10-MADSA and 9,10-PADSA) and 1-cyano-*trans*-1,2-bis-(4′-methylbiphenyl)ethylene (CN-MEB) by J-aggregate formation,[8–10] (iv) pyrene, cyanovinylene, and chrysene derivatives by excimer formation,[11,12] and (v) boron dipyrromethene (BODIPY) derivatives and barbituric acid-functionalized TPE derivatives (TPE-HPh-Bar) by twisted intra-molecular charge transfer (TICT),[13,14] and AIE glyconanoparticles by Förster resonance energy transfer (FRET).[15] Moreover, recent developments and advances of AIE molecules enable them to cover the entire visible spectrum and expand to the near-infrared range. Owing to the unique and intrinsic AIE property, AIE molecules have been usually employed for sensing applications that require high-resolution fluorescence imaging and long-term fluorescence tracking.

In parallel to the intrinsic aggregation nature of artificial AIE molecules, many naturally occurring proteins, regardless of their sequence, size, native structure, and biological function, have an inherent self-aggregation ability to form β-structure-rich fibrils (namely, amyloids), which are pathological hallmarks of
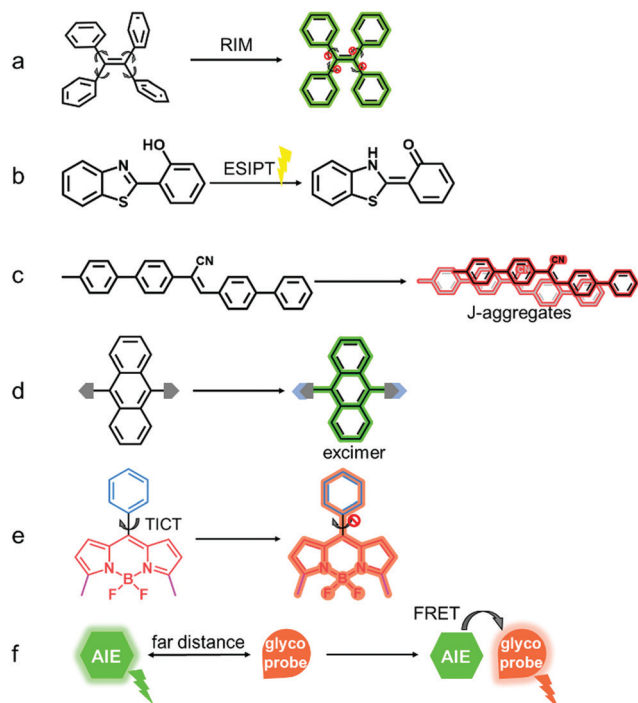
Fig. 1 Different AIE mechanisms of (a) RIM, (b) ESIPT, (c) J-aggregate formation, (d) excimer formation, (e) TICT (blue: donor groups and red: acceptor groups), and (f) FRET.

many neurodegenerative diseases, including Alzheimer's disease (AD), Parkinson's disease (PD), and type 2 diabetes (T2D). The β-sheet-rich amyloid aggregates are recognized as ideal biomarkers for developing new molecular ligands for therapeutic prevention and disease diagnosis. Fluorescent molecules, including organic dyes, inorganic nanoparticles, and fluorescent proteins, have been extensively developed and used as amyloid-binding ligands for elucidating the different aspects of amyloid aggregation, including (i) amyloid aggregation monitors; (ii) amyloid aggregation inhibitors or promoters, (iii) amyloid sensors and detectors, (iv) amyloid staining, imaging, and tracking, and (v) amyloid structure determinators.[16] Meanwhile, these fluorescent molecules always have their own disadvantages, which will limit their usage in certain situations. Specifically, organic dyes (e.g., thioflavin-T, Congo red, resveratrol, rifampicin, morin, and others) often contain many aromatic rings that usually cause the common ACQ effect, i.e., their fluorescence will be seriously quenched in the aggregation state, because intermolecular π–π interactions will exhaust the energy at the excited (binding or aggregation) states. Moreover, most of Thioflavin T (ThT), Congo Red (CR), and their derivatives tend to recognize β-structure-rich amyloid fibrils (e.g., less toxic or off-pathway species), but suffer from poor sensitivity to amyloid oligomeric aggregates that are considered as pathological species. Inorganic nanoparticles (e.g., quantum dots, carbon dots, nano-dots) usually contain heavy metals, chelation ions, or chalcogens, whose cytotoxicity to living cells is still hotly debated. An additional concern of nanoparticles is their agglomeration to cause the loss of fluorescence. Fluorescent proteins (e.g., green fluorescent

protein, GFP) generally achieve binding-induced fluorescence emission, which requires specific conformations for both fluorescent proteins and targets to bind and form a stable complex *via* spatial complementarity, dock-lock, and intermolecular non-covalent bonds.[17]

Different from those conventional fluorescent molecules that often possess the ACQ effect and are used at high concentrations for amyloid-related applications, the use of AIE to explore sequence/structure-dependent amyloid aggregation, inhibition, toxicity, and detection mechanisms appears to be an intuitive option at a first glance, because the AIE of fluorescent molecules and the self-aggregation property of amyloid proteins are a perfect match together through their functional complementarity. Surprisingly, although there has been a rapid growth in the number of publications on AIE in the past decade as evidenced by 9085 papers published in all research fields and 471 papers for protein detection since 2012 when searched with the keywords "aggregation-induced emission" and/or "protein" in the Web of Science, the literature search with the keywords "aggregation induced emission" and "amyloid" leads to only 23 publications (Fig. 2), indicating that the study of AIE molecules for disease-related protein aggregates is still at an infant stage with much less scientific exploration. On the other hand, despite the limited number of AIE–amyloid studies, AIE molecules have demonstrated their superior ability to effectively address the different issues of amyloid aggregation, including (i) general fluorescence response to a wide variety of amyloids (Aβ, insulin, α-synuclein, htt, HEWL) with high sensitivity, (ii) strong binding affinity (∼4 fold increase) to amyloids as compared to ThT (the most commonly used dye for amyloids), (iii) super high resolution (∼10 time resolution enhancement) to detect amyloid aggregates, (iv) diverse sensing capacity to detect toxic oligomers at the earlier stages of amyloid aggregation, (v) great expansion of amyloid systems from simple buffer solutions, organelles, cells, bacteria, tissues, to even animals, (vi) easy incorporation with other imaging techniques (e.g., Raman, CT, MRI, and PA) to achieve synergistic
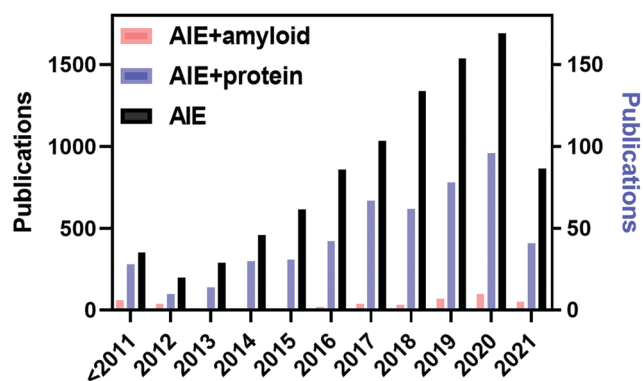
Fig. 2 Numbers of SCI-index papers for AIE-related studies between 2011 and 2021, when searched with the keywords "AIE", "aggregation induced emission", "protein", "amyloid", in the topics of papers from the Web of Science. Of note, publications searched with "AIE" are shown in the left axis, while publications searched with "AIE + protein" and "AIE + amyloid" are shown in the right axis.

This journal is © The Royal Society of Chemistry 2022

J. Mater. Chem. B, 2022, **10**, 2280–2295 | **2281**

imaging multimodalities. The presence of dominant aromatic rings in AIE molecules gives rise to high binding affinity to amyloids, the photo-luminescence "turn-on" characteristics, and a better signal to background ratio. Given the wide variety of amyloid aggregates from oligomers, protofibrils, to fibrils, conventional fluorescent molecules (*e.g.*, ThT, Congo red, and their derivatives) mostly or only recognize specific β-structure-rich aggregates, but AIE molecules are more amenable to identify these aggregated amyloids, independent of their sizes and structures, and thus they are shown to have superior photo-luminescence response. Further structural modifications of AIE derivatives *via* substitutions of different side groups in different positions (*e.g.*, QM-FN *vs.* QM-FN-SO$_3$[18]) endow them with improved fluorescence response and detection capacities both *in vitro* and *in vivo*, as well as with greater resistance to the nanoparticle-induced quenching effect. Another application of AIE molecules includes labeling them with amyloid proteins for real-time tracking and visualization of the extracellular and intracellular uptake and aggregation of amyloid formation. Currently, considerable studies have been done using AIE molecules as fluorescent probes for monitoring amyloid aggregation in the range of 400-680 nm, which have significant imaging limitation particularly for cell and tissue contrast. Development of NIR emissive AIE molecules in the range of 600–900 nm is highly desirable because of the better fluorescence imaging and the less fluorescence-induced toxicity for cells and tissues at much lower cost. Finally, less studies have discovered AIE molecules as inhibitors/promoters for modulating amyloid formation, probably due to their potential solubility and biocompatibility issues. Conjugation of AIE molecules with other functional materials (*i.e.*, peptides/proteins, carbohydrates, DNA/RNA, enzymes, nanoparticles) not only improves their water solubility and hydrophilicity, but also introduces new functions of biomarker detection, cancer targeting, and gene delivery. Thus, it is equally important for the structural design of new AIE molecules and further engineering/optimization of existing AIE molecules for studying amyloid aggregation, toxicity, inhibition, sensing, and imaging.

Different from several comprehensive reviews regarding AIE molecules for fluorescent sensors,[19] bioprobes for biomedicine,[20–24] sugar-based materials,[25] composite materials,[26] and photodynamic therapy,[27] this outlook mainly aims to provide the first summary of the developments and applications of AIE molecules for amyloid proteins, with a specific emphasis on the four types of AIE molecules and their applications for Aβ (associated with AD), insulin (associated with T2D), and α-synuclein (associated with PD) aggregates, including the detection, inhibition/promotion, and imaging of amyloid protein aggregates at the molecular, cellular, and animal levels. We acknowledge these early and pioneering AIE studies on amyloids, discuss joint working mechanisms for both AIE and amyloid aggregation, and give some perspectives of current challenges and future direction of AIE–amyloid systems, all of which will hopefully inspire more and continuous research efforts for exploring the full potentials of AIE in the biomedical field.

2. AIE interaction mechanisms with amyloid aggregates

Considering that amyloid formation is a complex, multiphase process, involving structural transition from unaggregated and unstructured monomers at a lag phase, to intermediate aggregates of oligomers/protofilaments at a growth phase, to finally highly aggregated, β-structure-rich amyloid fibrils at an equilibrium phase.[28–31] During this aggregation process, amyloid aggregates of different sizes and shapes also undergo complex structural misfolding, merging, and reorganization to form new species, making them very difficult to detect by any fluorescent molecules (not limited to AIE molecules). Depending on the compositions and structures of AIE molecules, while the exact AIE mechanisms to explain AIE–amyloid-binding-induced fluorescence emission are still under exploration and debate, different AIE mechanisms are proposed regarding the interaction of AIE molecules with amyloid aggregates, including RIM, TICT, and FRET.

Among them, RIM is considered as the main working mechanism to explain the AIE phenomenon. Upon amyloid aggregation under appropriate conditions, AIE molecules interact strongly with amyloid aggregates, mainly *via* (i) electrostatic attraction between oppositely charged AIE molecules and amyloid motifs/aggregates, (ii) specific structural recognition or complementarity between AIE molecules and amyloids using conjugated or substituted groups, (iii) hydrophobic interaction between the aromatic structure of AIE molecules and the hydrophobic pockets of amyloid aggregates, and (iv) chemical reactions to bond AIE molecules to amyloids (Fig. 3), which in turn restrict the intramolecular motions (rotations and vibrations) of AIE molecules. Next, the RIM of AIE molecules will decrease the dissipation of excited-state energy and block the nonradiative
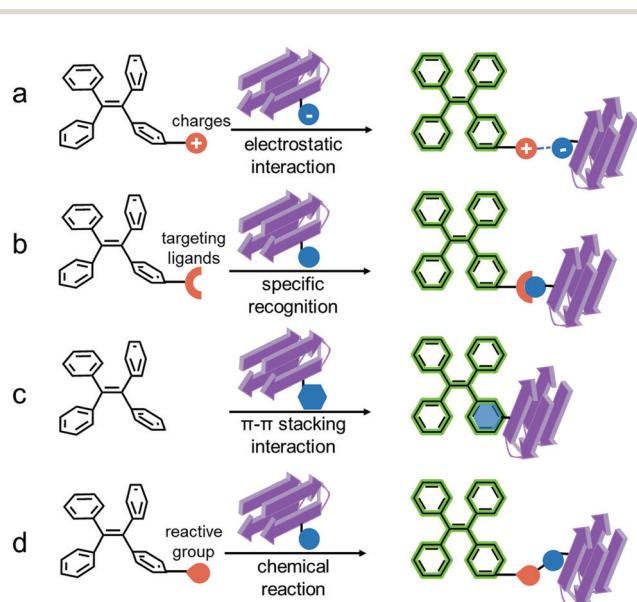

Fig. 3 AIE interaction mechanisms to recognize amyloid aggregates through (a) electrostatic attractions, (b) specific recognition and structural complementarity, (c) hydrophobic interactions, and (d) chemical reactions.

2282 | *J. Mater. Chem. B*, 2022, **10**, 2280–2295

This journal is © The Royal Society of Chemistry 2022

Table 1 A summary of different types of AIE molecules used for detecting amyloid aggregates

Type	AIE molecule	Analyte	Ex/Em (nm)	Detection range	AIE mechanism	Other	Ref.
TPE-based AIE	BSPOTPE	Insulin fibrils	350/~470	0–100 μM (0–5 μM)	RIM	$C_B = 10^5$ M inhibition	41
	TPE–TPP	α-Syn oligomers and fibrils	350/~480	5 μM	RIM	$K_D = 4.36$ μM	32
	TPE–TPP	Aβ oligomers, protofibrils, and fibrils	380/465 380/452 380/406	0–10 μM	RIM	$K_D = 8.93$ μM $C^D = 2$ μM	34
	TPE-RGKLVFFGR	Aβ fibrils	370/~500	0–7.5 μM	RIM	$C^D = 0.5$ μM	42
	TAE-type AIEgen (6a)	HEWL fibrils	360–520	0–20 μg mL^{-1}	RIM	$R = 40$ nm $C^D = 0.59$ nM	43
	TPE-MI	Htt in cell model	—	—	RIM	—	44
	EPB@α-syn EPB@Aβ	Amyloid inhibitors	350/480	—	RIM	—	45
Styrene-based AIE	DM-BZ	HEWL fibrils	365/~480	0–280 μg mL^{-1}	RIM	C^D (HEWL) = 152.86 nM	46
	PD-BZ	HEWL fibrils	365/~480	0–280 μg mL^{-1}	RIM	C^D (HEWL) = 87.64 nM	46
	PD-NA	HEWL fibrils Aβ fibrils	405/~520	0–280 μg mL^{-1}	RIM	C^D (HEWL) = 160.70 nM R (Aβ plaques) = 38 nm	46
	PD-NA-TEG	HEWL fibrils Aβ fibrils	405/~520	0–280 μg mL^{-1}	RIM	C^D (HEWL) = 63.71 nM R (HEWL) = 38 nm R (Aβ plaques) = 49 nm	46
	PD-BZ-OH	HEWL fibrils	—/596	30 μg mL^{-1}	RIM	$R = 35$ nm SF = 186 nm	47
	PyB-M	HEWL fibrils	494/~635	35 μM	RIM	—	36
	BG	Insulin fibrils	640/678	0–30 μM	RIM and TICT	$C^D = 0.34$ μM	48
	FA	Aβ fibrils Lipid droplets	—/570	0–10 μM	RIM	$C^D = 37$ nM	26
	FB	Aβ fibrils Lipid droplets	565/570	0–10 μM (0–5 μM)	RIM	$C^D = 26.9$ nM $K_D = 47.91$ nM SF = 140–180 nm	26
	Cur-N-BF$_2$	Aβ fibrils	426/565	20 μM	RIM and TICT	Inhibition	37
	ASCP	α-Syn oligomers and fibrils	460/605	0–50 μM	RIM	$K_b = 5.5$ μM $C^D = 0.5$ μM SF = 145 nm	49
	P1	SOD1-A4V oligomers and fibrils	540/640	5 μM	RIM and TICT	—	35
	P18	SOD1-A4V fibrils	450/520	5 μM	RIM and TICT	—	35
DSA-based AIE	AuNC@SiO$_2$-Apt-BSNVA	PrP^{sc}	410/540	0–200 nM (0–15 nM)	RIM	$C^D = 10$ pM	50
	BDVAI@AuNCs-Apt	Insulin fibrils	—/553	0–1000 nM (0–50 nM)	RIM	$C^D = 23.6$ pM	51
Others	DES DES-DKs	Aβ species	374/491 374/620	0–70 μM	RIM and FRET	—	15
	G3-biph-3	Insulin oligomers and fibrils	220/367	0–25 μM (0–25 μM)	RIM	—	52
	PTC1	Aβ fibrils	340/~415	0–6 μM	RIM	$C^D = 0.63$ μM $C_B = 6.63 \times 10^5$ M	53
	QM-FN-SO$_3$	Aβ fibrils	500/665	0-9 μM	RIM	—	18
	DPAPMI	Insulin fibrils	375/435	50 μM	RIM	SF = 130 nm acceleration	54
	CPMI	Insulin fibrils	375/420	50 μM	RIM	SF = 80 nm acceleration	54

C^D = minimal concentration of amyloids detected by AIE probes. K_D = dissociation constant of AIE probes with amyloids. C_B = binding constant of AIE probes with amyloids. R = resolution fluorescence imaging of amyloids. SF = Stokes shift as produced by AIE probes.

decay, thus triggering high luminescence in the aggregation (*i.e.*, amyloid binding) state. Moreover, such specific AIE–amyloid interactions and conformational restrictions are also sensitive to the surrounding environment, leading to a low background noise. Tetraphenylethene (TPE), cyanstyrene, 9,10-distyrylanthracene (DSA), and silole-diyne (DES) (Table 1 and Fig. 5) are the representative AIE molecules that demonstrate the RIM mechanism;

they are non-emissive as diluted or solvated species, because their excited-state energy is dissipated through the molecular motions of the aromatic rings; however, the strong binding of these AIE molecules to amyloid aggregates prevents the intermolecular motions so that the excited-state energy can only be released through radiative pathways. Since most RIM systems contain aromatic-based or conjugated hydrocarbons, heteroatoms, or

This journal is © The Royal Society of Chemistry 2022

J. Mater. Chem. B, 2022, **10**, 2280–2295 | **2283**

organometallics, the enhanced fluorescence is attributed to the restriction of molecular motions upon interacting with amyloid fibrils of different sequences. As an example, bis(triphenylphosphonium) tetraphenylethene (TPE–TPP) has demonstrated its superior fluorescence response to different aggregated forms of different amyloid proteins, including α-synuclein oligomers and fibrils,[32] α-lactalbumin ordered aggregates,[33] and oligomeric and fibrillar Aβ,[34] strong resistance to self-quenching, and high sensitivity to the most toxic oligomeric species, all of which are better than those of classical ThT.

However, some AIE molecules, particularly AIE-based conjugates, cannot be solely explained by the RIM mechanism. As a proof-of-example, a series of 4-hydroxybenzylidene-imidazolinone (HBI)-based AIEgens,[35] consisting of a donor and an acceptor linked by a single bond, possess TICT property, i.e., HBI-based AIE molecules undergo free rotation at the excited state to emit dark fluorescence due to nonradiative decay via TICT. In contrast, the free rotation of AIEgens can be gradually restricted due to the increased environmental viscosity, which will turn on fluorescence upon co-incubation with amyloids. A combination of RIM and TICT allows fluorescence sensitivity and intensity to be synergetically enhanced, as evidenced by barbituric acid (BA)-based AIE molecules[36] and Cur-N-BF$_2$.[37] A similar concept has also been applied to combine RIM and FRET mechanisms in the silole-diyne glyconanoparticle (DES-GNP) for enhancing ratiometric sensing, in which DES as an AIE molecule shows strong green fluorescence and GNP as a conjugation partner shows red fluorescence. As a result, DES-GNP greatly improved the detection sensitivity and strength for probing Aβ aggregates.[15]

In addition to the use of AIE-based molecules for amyloid detection, a few AIE-based molecules were also found to inhibit/promote amyloid aggregation. Since both "detection" and "inhibition/promotion" of amyloid aggregates by AIE-based molecules are essentially governed by similar/same AIE–amyloid interactions, it is not surprising to observe in a few studies that AIE-based molecules (e.g., BSPOTPE, DPAPMI, and CPMI) can function as both amyloid detectors and amyloid inhibitors/promoters for specific amyloid proteins, i.e., amyloid inhibitors could potentially function as amyloid detectors, and vice versa. From a thermodynamic viewpoint, when introducing AIE-based molecules to amyloid solution, intermolecular interactions between AIE molecules and amyloid aggregates will lead to the formation of AIE–amyloid complexes at the expense of amyloid monomers in solution, so that amyloid aggregation pathways and equilibrium phases are remodeled. Furthermore, AIE–amyloid interactions could be competitive, cooperative, or both found at different aggregation stages, and thus different AIE-based molecules can modulate amyloid aggregation at different stages by affecting (mis)folding structures, assembly pathways, toxic species populations, and membrane interactions of amyloid aggregates. Looking ahead, while there have been no reports on the role of AIE-based molecules in amyloid aggregation and toxicity, hypothetically, AIE-based molecules can (i) retain non-β-structure conformation of amyloid amorphous aggregates; (ii) redirect amyloid aggregation pathways by
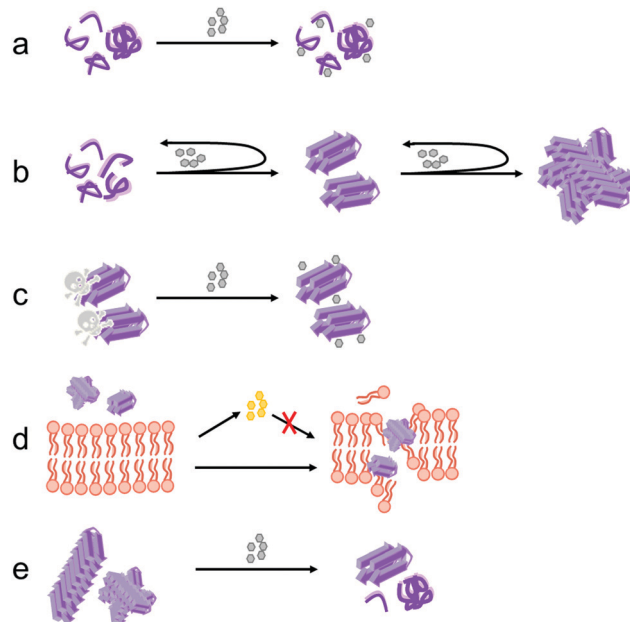

Fig. 4 Different hypothetical models for AIE-based molecules to modulate amyloid aggregation and toxicity by (a) retaining amyloid amorphous aggregates with no well-defined secondary structures, (b) redirecting amyloid aggregation pathways, (c) forming less-toxic AIE–amyloid complexes, (d) altering membrane interactions of AIE–amyloid complexes with cell membranes; and (e) disassembling the preformed amyloid aggregates.

modulating amyloid oligomerization but not amyloid fibrillization, or amyloid fibrillization but not amyloid oligomerization, or both; (iii) bind to amyloid aggregates to form more or less toxic AIE–amyloid complexes; (iv) alter the membrane interactions of AIE–amyloid complexes with cell membranes; and (v) disassemble the preformed amyloid aggregates. These facts and hypothetical scenarios may not necessarily exclude each other, implying that the interactions between AIE-based molecules and amyloid aggregates are far more complex than our expectation, but are key factors governing amyloid misfolding, aggregation, and toxicity (Fig. 4).

3. AIE-based molecules for amyloid protein aggregates

There are ~50 different amyloid proteins, including Aβ, α-syn, insulin, and htt, which are pathologically associated with different amyloid diseases.[38] It is known that most amyloid diseases are incurable, mainly because there are no effective and reliable diagnostic strategies for early detection of amyloid aggregates before preclinical and prodromal symptoms occur, at which stage significant and irreversible damage would have been done to the diseased organs, including the brain, eye, heart, liver, pancreas, and nervous system. Moreover, while fluorescent molecules (not limited to AIE molecules) have been extensively developed for the detection of amyloid aggregates, these fluorescent probes are mostly limited to a single-target or a single-mode detection, leading to high failure rates of these
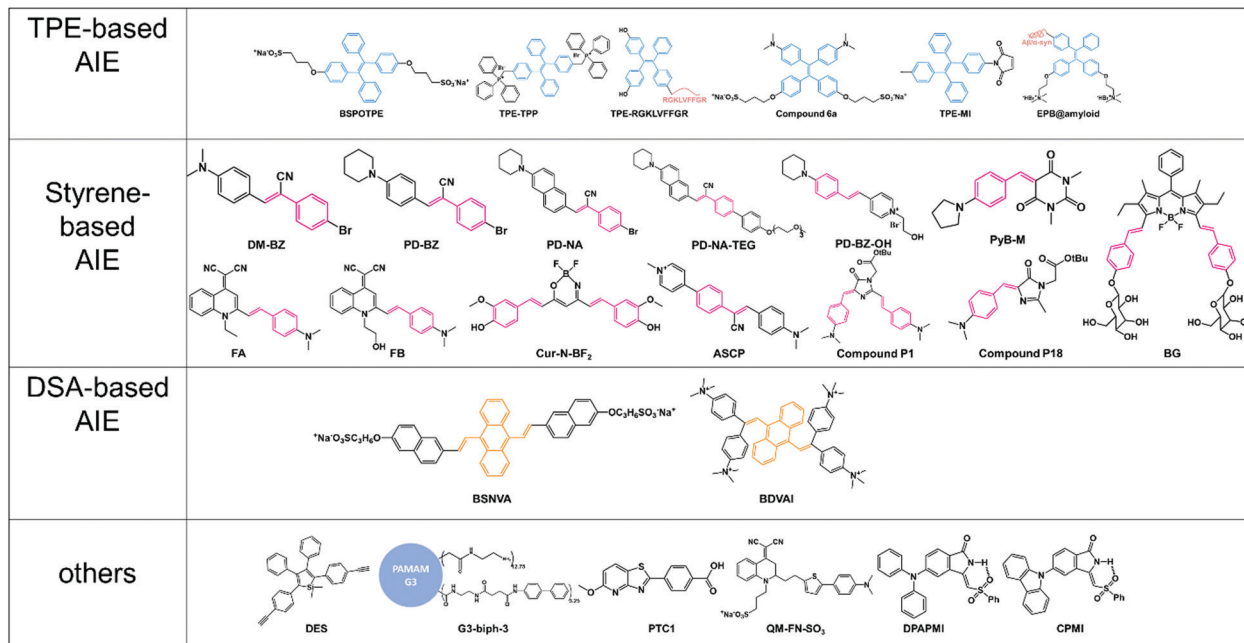
2284 | J. Mater. Chem. B, 2022, 10, 2280–2295

This journal is © The Royal Society of Chemistry 2022

Fig. 5 Chemical structures of four types of AIE molecules for amyloid aggregates.

amyloid probes in clinical trials.[39] More importantly, recent findings in amyloid cross-seeding (or ''proteinopathies'') show the prevalent co-existence and mixtures of different amyloid proteins in blood plasma and cerebrospinal fluids, in correlation with the co-occurrence of different amyloid diseases in the same individuals.[40] This fact indicates that single-target amyloid probes with single-mode detection would not be sufficient to detect different amyloid proteins that are pathologically linked to each other, thus adding another profound challenge for developing new multi-target/multi-mode AIE-based probes/sensors with improved sensitivity and selectivity for the detection of homo- and hetero-aggregates of different amyloid proteins. Here, we summarize and classify the AIE molecules in terms of their structures for detecting amyloid aggregates *in vitro* and/or *in vivo* in Table 1 and Fig. 5.

3.1.   Tetraphenylethene (TPE)-based AIE molecules

TPE, as one of the most well-known AIE-active luminogens, has a propeller-like structure bearing four phenyl rotors around a central olefin stator.[55] Such a structural feature endows TPE with AIE properties, emitting weak fluorescence in the dissolved state, but strong fluorescence in the aggregated state. In the dissolved state, the free rotation of the four phenyl rings in TPE provides a nonradiative relaxation pathway for excited electrons, thus resulting in nonfluorescence. However, upon aggregation, the RIM of these phenyl rings are triggered to release strong photoluminescence. The special structural characteristic of TPE allows it to be used as a template for the design of different TPE derivatives *via* (i) easy incorporation into different ACQ fluorophores to endow them with a new AIE characteristic and high emission efficiency[56,57] and (ii) convenient structural modification and functionalization by simple

reactions (*e.g.*, BSPOTPE, TPE-MI, and TPE–TPP) to meet the needs of different applications.[58]

Among TPE and its derivatives, a water-miscible TPE salt – sodium 1,2-bis[4-(3-sulfonatopropoxyl)phenyl]-1,2-diphenylethene (BSPOTPE)[41] – was first synthesized to possess dual functions as an (i) *ex situ* monitor (Fig. 6a) to detect insulin aggregation kinetics (associated with T2D) and (ii) *in situ* inhibitor against insulin fibril formation. Similar to other fluorescent molecules (*e.g.*, ThT, CR) for detecting amyloids, BSPOTPE can also not only detect a typical nucleation-polymerization aggregation profile of insulin including three distinct aggregation stages of insulin nucleation, growth, and equilibration, but also exhibit a linear relationship between emission intensity and insulin concentration in the region of 0–5 μM, allowing BSPOTPE to be further used as a quantitative probe for quantifying fibrillar insulin. Apart from its use as an insulin detector, BSPOTPE (100 μM) also functions as an amyloid inhibitor to significantly reduce insulin fibrillization (500 μM). As revealed by molecular dynamics (MD) and molecular docking simulations, both detection and inhibition functions of BSPOTPE stem from the strong and specific binding of the phenyl rings of BSPOTPE to the hydrophobic residues of insulin including leucine, valine, phenylalanine, and tyrosine.

As described above, amyloid oligomers are not only the most toxic species to induce cell cytotoxicity,[59] but also the intermediate species to continuously promote protein aggregation by converting amyloid monomers to amyloid fibrils.[60] Moreover, since amyloid oligomers always exhibit a wide variety of sizes, shapes, conformations, and probably even functions, the detection of these intermediate, dynamic, diverse amyloid oligomers by specific or general AIE-based molecules is undoubtedly critical yet challenging for the early diagnosis or potential treatment of
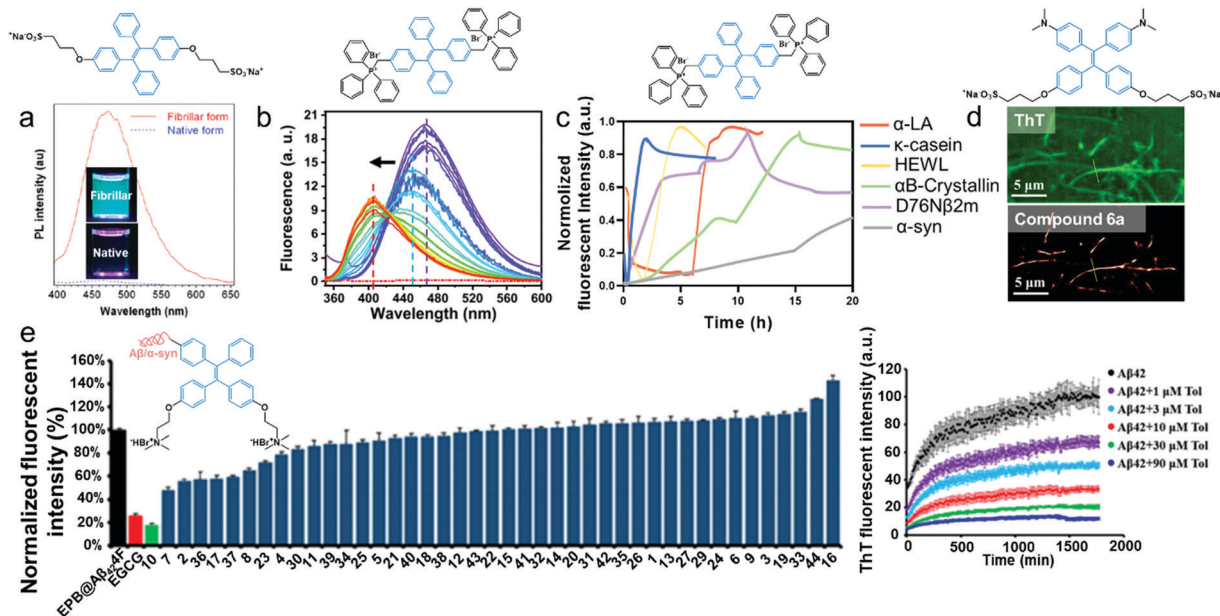
Fig. 6 TPE-based AIE molecules for amyloid detection, imaging, and inhibition. (a) BSPOTPE emits strong green fluorescence when detecting aggregated fibrillar bovine insulin, but no fluorescence for unaggregated native bovine insulin under a UV light of 365 nm. (Reprinted with permission,[41] Copyright © 2011 American Chemical Society.) (b) Fluorescence emission spectra of TPE–TPP to track three distinct aggregation intermediates of Aβ. (Reprinted with permission,[34] Copyright © 2020 American Chemical Society.) (c) TPE–TPP exhibits multi-target sensing ability to detect α-LA, κ-casein, HEWL, αB-crystallin, D76Nβ2m, and α-syn aggregates. (Adapted with permission,[33] Copyright © 2017 American Chemical Society.) (d) Compound **6a** shows super high resolution to image HEWL fibrils as compared to ThT. (Reprinted with permission,[43] Copyright © 2021 American Chemical Society.) (e) EPB@Aβ$_{42}$4F is designed as a screening platform to achieve a large-scale database searching for amyloid inhibitors against the aggregation of Aβ$_{42}$. (Reprinted with permission,[45] Copyright © 2020 American Chemical Society.)

amyloid diseases.[61,62] To this end, tetraphenylethene–triphenyl-phosphonium (TPE–TPP) was designed as a new fluorescent probe to recognize different amyloid oligomers of α-synuclein (associated with PD)[32] and Aβ (associated with AD).[34] As compared to traditional ThT, upon co-incubation with α-synuclein TPE–TPP not only displayed much more stronger fluorescence intensity, but also showed higher binding affinity to α-synuclein fibrils, both of which produced a higher fluorescence intensity and signal-to-background ratio. Besides, TPE–TPP showed a much earlier response (~18 h) to α-synuclein oligomers, in contrast to the late response of ThT (~30 h) to α-synuclein fibrils, demonstrating the high detection sensitivity and affinity of TPE–TPP for α-synuclein oligomers. In parallel, fabrication of TPE–TPP into a time-resolved fluorescence lifetime assay system allows Aβ oligomers of three distinct sizes and conformations to be traced using different emission wavelengths, including small oligomers with antiparallel β-sheets but without the formation of the D23–K28 salt bridge by using 465 nm wavelength, large oligomers/proto-fibrils with both salt bridges and parallel β-sheets by using 452 nm wavelength, and mature fibrils by using 406 nm wavelength[34] (Fig. 6b). The average trace fluorescence lifetime for the three types of Aβ oligomers was superfast, as evidenced by fluorescence lifetime values of 3.58, 3.00, and 5.19 ns, respectively. More impressively, TPE–TPP can also recognize the other prefibrillar/oligomeric aggregates of α-lactalbumin (α-LA), κ-casein, hen egg white lysozyme (HEWL, associated with familial lysozyme systemic amyloidosis), the recombinant

D76N variant of β2-microglobulin (D76Nβ2m, associated with haemodialysis-related amyloidosis), and αB-crystallin (associated with cataract)[33] at even an acidic pH of 2 and a high temperature of 60 °C (Fig. 6c). Such general amyloid recognition ability of TPE–TPP is attributed to the unique structural combination of TPE as a fluorescent probe and TPP as an amyloid targeting moiety, enabling it to distinguish different amyloid species.

On the other hand, multi-target AIE probes, despite their super general detection ability, often suffer from poor selectivity, which greatly limits their practical applications. To address this issue, a new design strategy is to conjugate TPE with a specific recognition peptide RGKLVFFG selected from the central hydrophobic core of Aβ. Due to the sequence homology, it is not surprising to observe that TPE-RGKLVFFG[42] was nonfluorescent when co-incubated with non-aggregated Aβ monomers, but switched on its fluorescence by TPE upon specific binding of RGKLVFFGR to similar sequences and β-sheet-rich structures of Aβ$_{40}$ fibrils. TPE-RGKLVFFG not only emitted ~4-fold stronger fluorescence than ThT, but also showed high resistance to the nanoparticle-induced ACQ effect.

Seeing is understanding. While many of the aforementioned TPE-based AIE molecules have been developed to detect different types of amyloid aggregates, the high-resolution optical visualization of amyloid fibrils by these AIE molecules is rarely reported. Recently, a series of water-soluble AIE-active tetraarylethenes (TAE-type AIEgens) with different types of alkylamino substituent groups were successfully synthesized to show the super-resolution

imaging of HEWL aggregates[43] upon AIE activation. This design considers the introduction of (i) a *N,N*-dimethyl amino group with high electron-donating capability for activating the aromatic ring of AIE molecules by increasing the electron density on the ring and (ii) hydrophilic, negatively charged sulfonate anions to increase both water solubility *via* ionic solvation and binding affinity *via* electrostatic interactions. Among them, compound **6a** containing sulfonate and *N,N*-dimethyl amino groups exhibited the highest sensitivity for detecting HEWL fibrils, as evidenced by the lowest detection limit of 0.59 nM and the super high-resolution fluorescence imaging at 43.8 nm (Fig. 6d).

Apart from the utilization of TPE-scaffold AIE molecules as amyloid probes, we developed a new amyloid inhibitor screening system by site-specific conjugation of AIE molecules (EPB) with Aβ or α-synuclein proteins (*i.e.*, AIE@amyloid probes) to realize a high-throughput screening of small-molecule inhibitors against Aβ and α-synuclein aggregation.[45] By optimizing site-conjugation positions, the resultant AIE@Aβ and AIE@α-synuclein retained their amyloidogenic properties, and thus they emitted strong fluorescence due to their self-aggregation, but showed no fluorescence in the presence of amyloid inhibitors due to the prevention of amyloid aggregation. Using this working principle, we applied both AIE–amyloid probes as a screening platform to conduct a large-scale search from a small-molecule database containing 1742 compounds for general amyloid inhibitors against the aggregation of both Aβ and α-synuclein (Fig. 6e). Throughout the systematic search, tolcapone was found to inhibit the aggregation of both Aβ and α-synuclein, reduce the cytotoxicity of Aβ- and α-synuclein-induced aggregations in living cells, and improve the spatial cognition and objective recognition of the Aβ-treated mice. This work, from a different viewpoint, demonstrates a new design principle that both "inhibition" and "detection" of amyloid aggregates require the same/similar strong β-sheet interactions to occur between ligands and amyloids, *i.e.*, amyloid inhibitors could potentially function as amyloid detectors, and *vice versa*.

From a clinical viewpoint, proteostasis is a chronically imbalanced process and co-involved in the onset and development of amyloid diseases. To measure proteostasis imbalance in the context of amyloid diseases, tetraphenylethene maleimide (TPE-MI)[44] was developed and used as an on-demand fluorescent probe for detecting cellular misfolded protein load. The underlying working principle of TPE-MI is simply based on the naturally occurring folding and unfolding process of any protein. Under physiological conditions, proteins are biologically folded where cysteine thiols are mainly buried in the core of folded proteins. However, under disease conditions, misfolded proteins expose their cysteine thiols that can be specifically recognized by TPE-MI *via* the maleimide. In this way, TPE-MI allows one to quantify the extent of unfolded Huntington protein and determine its proteostasis imbalance level in Huntington disease using pluripotent stem cell models.

3.2. Styrene-based AIE molecules

Styrene-based AIE molecules contain a linear and planar spatial structure of styrene group, in which the styrene can freely rotate in the unrestricted solution state, but it can also insert into the β-sheet structure of amyloid aggregates to induce RIM and emit strong fluorescence. Meanwhile, based on the styrene scaffold, the cyano group is frequently inserted as a substitute group into "C=C" bonds to modify styrene-based molecules for improving the AIE emission capacity through (i) steric repulsion between cyano substituents and phenyl rings, (ii) intermolecular and intramolecular hydrogen bonds (*i.e.*, C–H···N), and (iii) electrostatic interactions.[63,64] Guided by these design strategies, a series of cyanostyrene-active AIE molecules[46] with piperidine (PD) or dimethylamino (DM)-substitutes at *para*-benzene (BZ) positions, which function as electron donating groups and specific amyloid binding groups, were synthesized to examine their capacity for detecting and imaging amyloid aggregates. The two molecules PD-BZ and DM-BZ demonstrated their distinct luminescence characteristics to show individual blue and green color in their aggregated states. Structural substitutions of the benzene ring with the naphthalene (NA) ring render PD-NA and PD-NA-triethylene glycol (TEG) with better structural rigidity and integration, thus leading to higher photoluminescence property compared to that of BZ derivatives. Consequently, all of the four cyanostyrene-active molecules were able to differentiate native (non-aggregated) and fibrillar (aggregated) HEWL proteins with amyloid detection sensitivity in the order of PD-NA-TEG > PD-BZ > DM-BZ > PD-NA. Due to the highest AIE characteristics, PD-NA-TEG also showed fluorescence imaging of HEWL fibrils at a high resolution of ∼38 nm. More importantly, the four AIEgens, particularly PD-NA and PD-NA-TEG, were able to identify Aβ plaques in the lesion tissue of mouse brains. The extraction of Aβ plaques from mouse brain slices was further imaged to show typical amyloid fibrillar morphologies (Fig. 7a). In addition to the static super-resolution imaging of amyloid fibrils, PD-BZ-OH fluorophores can *in situ* visualize the dynamic evolution process of HEWL amyloid fibrillation starting from scattered small dots to short and long matured fibrils, with a nanoscale resolution of 35 nm[47] (Fig. 7b). Such dynamic super-resolution imaging of PD-BZ-OH fluorophores mainly stems from their reversible binding/unbinding affinity to the β-sheet structure of HEWL, thus leading to dynamic binding/unbinding-induced switching on/off of fluorescence.

To date, while different AIE probes have been reported for monitoring amyloid fibrillization, most of them emit green/blue fluorescence whose short-wavelength emission can penetrate deeply into the tissues to cause potentially severe damage.[65] Multicolor AIE molecules and the underlying AIE mechanisms are still rarely reported. It is still worthy and challenging to develop AIE fluorescent molecules for amyloid aggregation with emission in the near infrared (NIR) region. The common strategy is to incorporate long-wavelength emission compounds into AIE fluorophores to achieve both functions. Organic fluorescent dyes including barbituric acid (BA)-based molecules[36] and glucose-conjugated BODIPY (BG),[48] both of which consist of electron-donating aniline groups and electron-withdrawing groups, were designed to broaden the fluorescent spectral range for amyloid applications. Due to
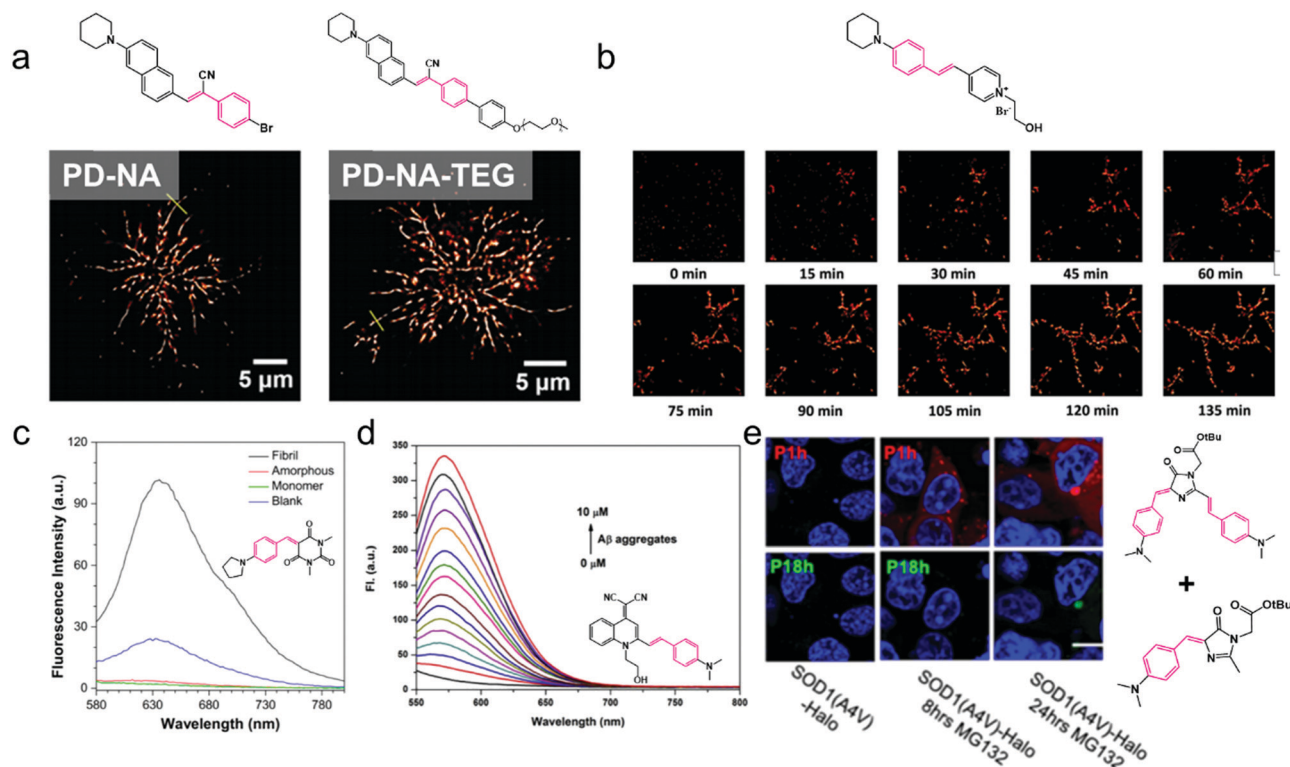
This journal is © The Royal Society of Chemistry 2022

J. Mater. Chem. B, 2022, **10**, 2280–2295 | **2287**

Fig. 7 Styrene-based AIE molecules for amyloid detection, imaging, and inhibition. (a) PD-NA and PD-NA-TEG possess super-resolution imaging of Aβ deposits in the brain slices of a Tg mouse. (Reprinted with permission,[46] Copyright © 2018 the Partner Organisations.) (b) PD-BZ-OH fluorophores can *in situ* visualize the dynamic evolution process of HEWL amyloid fibrillation starting from scattered small dots to short and long matured fibrils by super-resolution imaging. (Reprinted with permission,[47] Copyright © 2020 American Chemical Society.) (c) PyB-M exhibits distinct fluorescence emission when bound to different monomeric, amorphous, and fibrillar HEWL aggregates. (Reprinted with permission,[36] Copyright © 2020 MDPI (Basel, Switzerland).) (d) FB displays specific binding to Aβ aggregates within the range of 0–10 μM. (Reprinted with permission,[26] Copyright © 2020 Elsevier B.V.) (e) AggFluor (P1–P18) compounds exhibit differential turn-on fluorescence when bound to SOD1-A4V-Halo monomers (0 h), oligomers (8 h), and fibrils (24 h). (Reprinted with permission,[35] Copyright © 2020 American Chemical Society.)

the planar structure and strong electron-withdrawing ability of BA moieties, all these BA-based molecules displayed long-emission wavelengths in the orange-to-red region with typical AIE characteristics. Among ten BA-based molecules, PyB-M emitted strong fluorescence upon interacting with HEWL fibrils, but no fluorescence response to HEWL monomers, indicating that PyB-M can distinguish highly aggregated species of HEWL fibrils from unaggregated HEWL monomers[36] (Fig. 7c). In the case of the BG molecule, two styryl moieties were introduced into the BODIPY pyrrole rings to extend the conjugation and its emission wavelength towards the NIR region, while two sugar units were attached to the styryl moieties of BODIPY for better interactions with cellular membranes. The resultant BG molecules are not only capable of detecting both insoluble fibrils and soluble oligomers of insulin, but are also capable of *in vivo* imaging insulin plaques.[48]

In contrast to single-target amyloid probes, multi-target (multimodal) amyloid probes for detecting different biomarkers of the same or different amyloid diseases have several fundamental and technical advantages for early diagnosis and innovative therapeutics of these diseases.[66] A dual-functional AIE fluorescent probe named FB[26] was designed and synthesized by attaching a hydroxyethyl group to the nitrogen atom

of FA,[67] which possessed a classical donor–π–acceptor (D–π–A) architecture for AIE characteristics. The resultant FB exhibited not only high selectivity and binding affinity to Aβ aggregates with a detection limit as low as 26.9 nM (Fig. 7d), but also remarkable turn-on fluorescence enhancement for imaging the two AD-related biomarkers of Aβ plaques and lipid droplets at the cellular level and in brain sections of transgenic AD mice. Further molecular docking results showed that FB was able to plug into the hydrophobic pocket of Aβ$_{16–20}$ (KLVFF) to trigger intense fluorescence. The additional advantages of FB including the improved water solubility and blood–brain barrier (BBB) permeability ($\log P = 2.6$) allow it to serve as a structural template to design a series of FB derivatives with similar multi-target functions for early diagnosis and innovative therapeutics of AD and other amyloid diseases.

Another common strategy is to discover and design AIE fluorescence alternatives by structural modifications of traditional ThT, CR, and curcumin. Curcumin was re-designed into Cur-N-BF$_2$ by introducing BF$_2$ as a substitute into the ketone groups.[37] Cur-N-BF$_2$ not only avoids the ACQ effect, but also retains the original functions of curcumin for amyloid detection, inhibition, and elimination. Specifically, as compared with conventional ThT and curcumin, Cur-N-BF$_2$ as an amyloid detector

2288 | *J. Mater. Chem. B*, 2022, **10**, 2280–2295

This journal is © The Royal Society of Chemistry 2022

significantly enhanced fluorescence intensity even at a high concentration of 4 mM, but still retained high binding selectivity and affinity to Aβ fibrils in brain slices from a mouse model. As an amyloid inhibitor, a low dose of Cur-N-BF$_2$ (10 μM) can even disaggregate preformed Aβ fibrils (20 μM) and protect neuronal cells from Aβ-induced cytotoxicity by increasing cell viability from 55.5% to 83.2%. α-Cyanostilbene derivatives (ASCPs),[49] as a potential alternative to ThT, contain methyl pyridinium and dimethylamine moieties in the α-cyanostilbene core, which endows ASCPs with a large Stokes shift of 154 nm for simultaneously visualizing the fluorescently labelled proteins and ASCP-stained α-syn fibrils using total internal reflection fluorescence (TIRF) microscopy with only a single incident laser. Meanwhile, ASCPs were able to detect different forms of α-syn fibrils and amorphous aggregates, but they bound to α-syn fibrils much stronger than to α-syn amorphous aggregates.

Compared to extensive studies on Aβ, α-synuclein, and insulin, SOD1-A4V aggregation (associated with amyotrophic lateral sclerosis, ALS) is a relatively less-explored system. To visualize this multi-step aggregation process, a series of new fluorescent AggFluor compounds (P1–P18),[35] based on the chromophore rotor of GFP, were developed to span a wide range of viscosity sensitivity for detecting folded proteins, misfolded oligomers, and insoluble fibrils. All of these AggFluor (P1–P18) compounds turned on distinct fluorescence when bound to different SOD1-AV4 aggregates being formed at different aggregate stages. As a proof-of-example, a combination of both P1 and P18 enabled one to distinguish unfolded SOD1-AV4 monomers by dark color as induced by both P1 and P18, oligomers by red fluorescence as induced by P1, not P18, and fibrils by red fluorescence as induced by P1 and green fluorescence by P18 (Fig. 7e). Such a dual-color imaging feature is attributed to the different activation threshold according to the environmental viscosity/rotation angle. The abovementioned studies of different AIE molecules for amyloid detection and inhibition reveal a general working principle that amyloid detection and inhibition by AIE stem from a similar or the same origin of AIE–amyloid interactions, which lead to different effects on detection characteristics (i.e., brightness, electricity, and thermodynamics) or inhibition performances (amyloid structural folding, transition, and aggregation).

3.3. Distyrylanthracene (DSA)-based AIE molecules

9,10-Distyrylanthracene (DSA) often serves as a common AIE scaffold to derive DSA derivatives with enhanced AIE characteristics and distinct functions.[68] In DSA, chemical connection of multiple phenyl peripheries to an anthracene core through rotatable C–C bonds allows a large steric hindrance to be introduced between the anthracene core and peripheral groups, which will cause a large structural distortion in the DSA skeleton from a conjugate plane to a nonplanar structure via the RIR-induced AIE mechanism.[69,70] To enhance fluorescence intensity, plasmon-enhanced fluorescent (PEF) sensors, including metal nanoparticles (NPs), are often incorporated into the DSA backbone to largely increase the electromagnetic (EM) field for signal amplification. Despite few studies on DSA-based AIE molecules applicable to amyloid systems, hybrid PEF-AIE sensors[50] were designed to differentiate disease associated prion protein (PrP^{Sc}) from normal prion protein (PrP^C) by integrating three components together via (i) Au nanocubes (Au NCs) coated with silica (Au@SiO$_2$) as the PEF matrix, (ii) AIE molecule of 9,10-bis[2-(6-sulfonatopropoxy)naphthylethenyl]anthracene (BSNVA) as a fluorescent molecule, and (iii) aptamer of BSNVA on Au@SiO$_2$ as a specific recognition motif for PrP (associated with prion disease) (Fig. 8a). As expected, the resultant AuNC@SiO$_2$-Apt-BSNVA sensors did not emit fluorescence in solution alone and in the presence of PrP^C due to the lack of binding between BSNVA and PrP^C. In contrast, when co-incubating AuNC@SiO$_2$-Apt-BSNVA with PrP^{Sc}, BSNVA can bind specifically and strongly to PrP^{Sc} through hydrophobic interactions, leading to an obvious AIE-induced fluorescence enhancement with a detection limit of
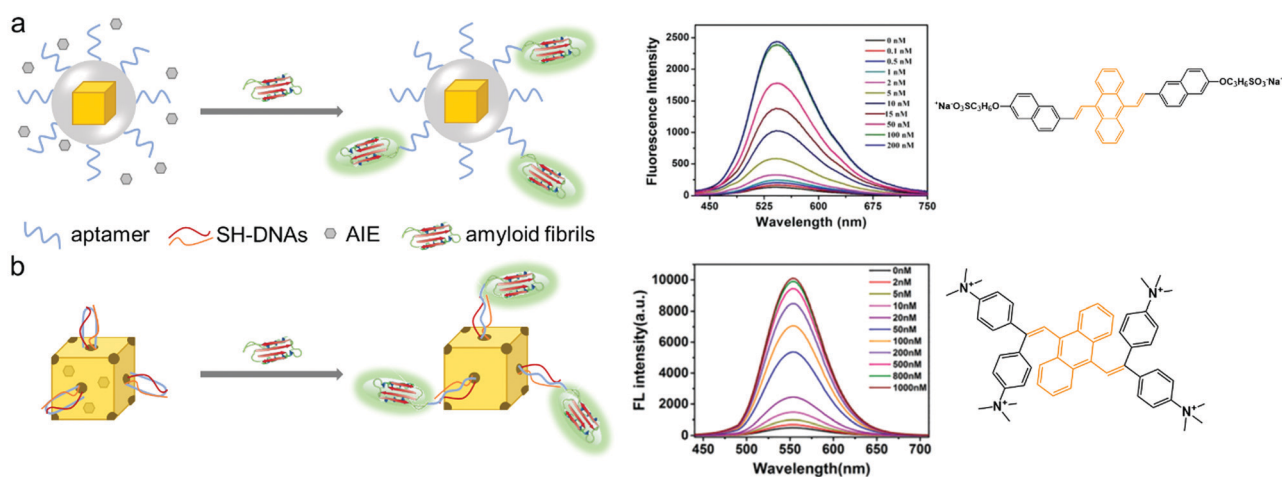
Fig. 8 DSA-based AIE molecules for amyloid detection and imaging. Design strategy and amyloid detection of (a) AuNC@SiO$_2$-Apt-BSNVA for PrP^{sc} aggregates (reprinted with permission,[50] Copyright © 2019 Wiley-VCH Verlag GmbH & Co. KGaA, Weinheim) and (b) AuNCs@DNA–BDVAI for insulin aggregates (reprinted with permission,[51] Copyright © 2021 The Royal Society of Chemistry).

This journal is © The Royal Society of Chemistry 2022

J. Mater. Chem. B, 2022, **10**, 2280–2295 | **2289**

PrP^{Sc} aggregates at 10 pM, demonstrating that the system was ~100 times more sensitive than BSNVA assay alone. This sensor was further utilized for detecting PrP^{Sc} in human serum samples. The AIE working mechanism of AuNC@SiO_2-Apt-BSNVA sensors can be explained by molecular docking results which revealed that the strong binding of BSNVA to the β-sheet structure of PrP^{Sc} leads to the RIM or RIR of BSNVA, thus switching on the enhanced fluorescence emission. This also explains the experimental observation that the lack of β-sheet structure of PrP results in nearly non-emissive fluorescence.

Very recently, a new water-soluble anthracene derivative with AIE property was synthesized by the same lab using a similar design strategy by integrating together gold nanocages (AuNCs) as a PEF enhancer, a modified DNA aptamer as a protein binding motif, and (anthracene-9,10-diylbis(ethene-2,1,1-triyl)) tetrakis (N,N,N-trimethylbenzenaminium)iodide (BDVAI) as an AIE molecule[51] (Fig. 8b). The resultant AuNCs@DNA-BDVAI enabled one to monitor the conformational change of the insulin fibrillization process, with a detection limit of fibrillar insulin at 23.6 pM. The unique structural design of AuNCs@DNA-BDVAI could trap DNA-BDVAI into and release DNA-BDVAI from the cage of AuNCs in the absence and presence of insulin fibrils. When insulin was presented, the strong binding of DNA to insulin will compete with the hybridization between SH-DNAs and the aptamer, causing AuNC cages to open, release BDVAI from the cages, and thus turn on significant fluorescence emission. So, the underlying AIE mechanism is that the released BDVAI strongly binds to the β-sheet structure of fibrillar insulin via hydrophobic interactions, which restricts the intramolecular rotation of BDVAI to turn on fluorescence.

3.4. Miscellaneous AIE molecules

In addition to the abovementioned AIE molecules discovered in the early studies, other AIE molecules with diverse structures have also been developed with enhanced AIE characteristics and additional functions. To date, most of AIE molecules for detecting amyloids are based on a fluorimetric response (i.e., fluorescence intensity), a direct indicator of AIE detection sensitivity. On the other hand, AIE-induced signal intensity is usually disturbed in complicated biomedia (e.g., blood serum/plasma, spinal fluids, and extracellular fluids). To address this issue, several silole-based AIE glyconanoparticles (AIE-GNPs)[15] were synthesized via supramolecular complexation between silole-diyne (DES) as AIE molecules and glycoprobes (DK1 and DK2) as nanoparticles to enhance Förster resonance energy transfer (FRET) between DK1 and DK2. AIE-GNPs were able to sensitively and selectively detect not only $A\beta_{42}$ and $A\beta_{40}$ of monomeric and fibrillar forms, but also lectins over a panel of other unselective lectins (N-acetyl glucosamine-selective wheat germ agglutinin, N-acetyl galactosamine-selective soybean agglutinin, and fucose-selective Ulex europaeus lectin 1) and proteins (pepsin, bovine serum albumin, ribonuclease A, lysozyme, and cytochrome c) by different ratiometric responses (Fig. 9a).
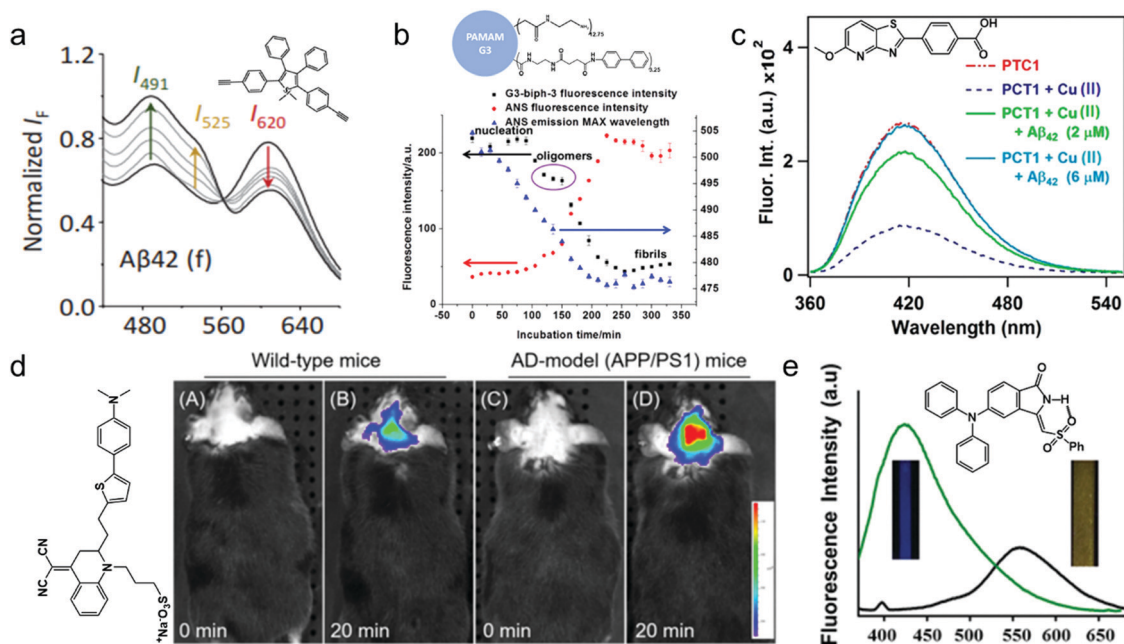

Fig. 9 Miscellaneous AIE molecules for amyloid detection and imaging. (a) AIE-GNPs (2×10^{-6} DES with 1×10^{-6} DK1) exhibit the size-dependent of Aβ42 aggregates on AIE fluorescence intensity. (Reprinted with permission,[15] Copyright © 2016 Wiley-VCH Verlag GmbH & Co. KGaA, Weinheim.) (b) G3-biph-3 monitors the aggregation process and structural transformation of insulin fibrillization. (Reprinted with permission,[52] Copyright © 2017 American Chemical Society.) (c) PTC1 displays reversible fluorescence quench in the presence of Cu^+ ions and fluorescence recovery in the presence of Aβ fibrils. (Reprinted with permission,[53] Copyright © 2019 American Chemical Society.) (d) QM-FN-SO3 lights up NIR fluorescence to the in vivo image Aβ plaques in APP/PS1 transgenic mice. (Reprinted with permission,[18] Copyright © 2019 American Chemical Society.) (e) DPAPMI organic dot switches on and switches off the fluorescence in the presence and absence of insulin fibrils. (Reprinted with permission,[54] Copyright © 2020 The Royal Society of Chemistry.)

2290 | J. Mater. Chem. B, 2022, 10, 2280–2295

This journal is © The Royal Society of Chemistry 2022

Different from inorganic-based AIE molecules, a series of AIE-grafted dendrimers with different grafting ratios -poly-amidoamine dendrimers (PAMAM) of generation 3 (G3) and generation 4 (G4) were conjugated with 4-aminobiphenyl (AIE molecule).[52] Considering the high binding affinity and diverse binding modes between dendrimers and insulin, AIE-grafted dendrimers can exhibit different binding affinities to insulin aggregates of different sizes. Specifically, G3-biph-3 can monitor the aggregation process and structural transformation from native insulin to oligomers and from insulin oligomers to fibrils (Fig. 9b). The larger insulin aggregates tend to form a looser packing with grafted PAMAM, thus causing different fluorescence.

Unlike the use of tetraphenylethene (TPE) and hexaphenyl-silole (HPS) as common AIE scaffolds for designing new AIE derivatives, a new aggregation-induced, emission-enhanced (AIEE) molecule 4-(5-methoxy-thiazolo[4,5-b]pyridin-2-yl)benzoi-cacid (PTC1)[53] was designed by structural modification of the pyridothiazole scaffold *via* replacement of the benzothiazole moiety with the methoxy-substituted pyridothiazole group. PTC1 demonstrated its ability for sensitive detection and monitoring of Aβ aggregation in a size-dependent manner, *i.e.*, PTC1 induced stronger fluorescence with the increase in the size of Aβ aggregates. More interestingly, the fluorescence of PTC1 can be reversely quenched in the presence of Cu^+ metal ions due to the disruption of PTC1 aggregates, but recovered after adding amyloidogenic Aβ fibrils due to the re-self-assembly of PTC1 aggregates (Fig. 9c). This further confirms that the quenching and regeneration of PTC1 fluorescence are attributed to dis-aggregation and aggregation-induced emission, respectively.

The design of AIE probes with extended wavelength to the NIR region is a more preferential strategy to obtain superior spatiotemporal resolution, maximize the photostability, and reduce potential tissue damage. To this end, a NIR AIE-active probe, QM-FN-SO_3, was designed by modifying the ACQ probe DCM-N with a lipophilic π-conjugated thiophene-bridge for extending the wavelength to the NIR region.[18] The QM-FN-SO_3 probe could function as a light-up NIR fluorescent probe upon binding to Aβ plaques in both *ex vivo* and *in vivo* AD-model mice (Fig. 9d), showing high signal-to-noise ratios over other conventional ThT and ThS probes. Another advantage of QM-FN-SO_3 is that it possessed desirable biocompatibility and BBB permeability when *in vivo* NIR imaging Aβ plaques. Thus, a unique structural combination of the lipophilic π-conjugated thiophene-bridge, quinoline-malononitrile (QM), and the sulfonate group in QM-FN-SO_3 can significantly reduce "false-positive" signals from the initial aggregation of AIE probes before binding to Aβ plaques.

Organic dots are well-known for their light-emitting properties. A series of promising photo-switchable AIE organic dots (DPAPMI, CPMI) were designed to study the aggregation kinetics of insulin fibrillization.[54] Consequently, both DPAPMI and CPMI can effectively probe insulin fibrils with a large hypsochromic shift and stain insulin fibrils for further bio-imaging (Fig. 9e), during which AIE dots are disassembled and coated on the hydrophobic surface of the fibrillar matrix and thus induce fluorescence. Moreover, DPAPMI and CPMI can also modify the insulin fibrillization pathways by accelerating the secondary nucleation and elongation process, with enhanced fluorescence emission. Different from conventional AIE molecules with large sizes that have difficulty crossing the BBB, AIE organic dots have advantages for BBB penetration, but organic AIE dots are required to be further tested and optimized for their biocompatibility and cytotoxicity. Overall, a systematic survey of all of AIE systems indicates that the integration of a light-up AIE characteristic in synergy with tunable aggregation behaviors will make a breakthrough to directly probe, image, and modulate amyloid aggregates and toxicity.

4. Conclusions and perspectives

Seeing is understanding. Apart from traditional fluorescent molecules, the past decade has witnessed the growing advancement in using AIE molecules for a wide variety of applications in the sensing, detecting, and imaging fields, due to their unique prominent advantages of high sensitivity, superior spatiotemporal resolution, rapid on-demand response, and noninvasive attributes. Particularly, the design and use of AIE molecules for disease-related protein aggregation are fundamentally important not only for a better mechanistic understanding of protein aggregation *in vitro* and *in vivo* from different aspects, but also for the high clinical benefits of prevention strategies of these protein aggregation diseases. But, a large majority of studies have focused on the design and use of AIE-based molecules as amyloid probes, in contrast to less studies exploring the other functions of AIE-based molecules as amyloid aggregation modulators, drugs, and treatments/therapies, probably due to complicated AIE–amyloid interactions and unknown reasons, including poor biocompatibility, low solubility, weak binding affinity and selectivity, and/or low permeability across the blood–brain barrier (BBB). Thus, there is still a large room to discover new functions of AIE-based molecules, reveal many unexamined AIE–amyloid scenarios, and explore their transformative potential for diverse applications in disease diagnosis, health monitoring, damage/motion detection, water/food safety, and environmental monitoring.

First, from a structural design viewpoint, the number of AIE molecules used for amyloid proteins is still rather very limited, due to complex synthesis routes, poor water solubility, and uncertain cell toxicity. Most of the commonly used AIE molecules are still largely based on the modification of TPE and silole motifs. The first priority of developing new AIE molecules is to expand the family of AIE molecules with enhanced fluorescence efficacy and multiple functionalities. Moreover, introducing new or multiple functions in AIE molecules *via* structural modifications remains to be explored. There are two strategies to structurally modify and functionally repurpose pure AIE molecules: (i) group substitutions to obtain AIE derivatives and (ii) molecular conjugations to obtain AIE conjugates. The design of AIE derivatives is a common and straightforward strategy, *i.e.*, simple brute-force substitutions

This journal is © The Royal Society of Chemistry 2022

J. Mater. Chem. B, 2022, **10**, 2280–2295 | **2291**

of most potentially questionable groups of AIE molecules with hydrophilic and charged groups will be systematically applied to screen and obtain the optimal AIE derivatives. Alternatively, introducing different molecules (*i.e.*, proteins/peptides, DNA/RNA, carbohydrates, nanoparticles) into the existing AIE molecules *via* chemical bonds or physical associations endows the resultant AIE conjugates with improved water-solubility, biocompatibility, and binding specificity/affinity, while still retaining their high AIE property. Another important advantage of AIE conjugates is introduction of new functions from the conjugated counterpart or integration of the merits of both AIE and conjugated counterparts, *i.e.*, cell targeting, dual-modality, superior cellular retention, good theranostics, and intense luminescence. Apart from the AIE characteristic, expansion from pure AIE to AIE derivatives and conjugates can greatly increase the family of AIE-based molecules of different compositions and structures. Additionally, dominant aromatic rings in AIE molecules present a double-edged sword: on the one hand, the dynamic regulation of these aromatic rings *via* AIE–amyloid π–π and hydrophobic interactions endows them with unique AIE character; on the other hand, aromatic rings also introduce high structural hydrophobicity, making them prone to self-aggregation and show poor solubility, both of which will severely compromise their fluorescence responses to amyloid aggregates in aqueous environments. Increasing the water solubility of AIE probes allows them to maintain good miscibility in biological media and achieve the off–on fluorescence during the amyloid aggregation process for high sensitivity and fidelity. AIE derivatives and conjugates are possible solutions to address these issues. Another challenge for designing AIE conjugates is to avoid fluorescence quenching caused by unknown conjugated counterparts in real complex media from different sources (*e.g.*, PBS solutions, spinal fluids, cells, tissues).

From an amyloid viewpoint, it is generally accepted that soluble amyloid oligomers, rather than initial amyloid monomers or final insoluble amyloid fibrils, are toxic species, thus developing new AIEs, AIE derivatives, and AIE conjugates, capable of recognizing and responding to amyloid oligomers, is critically important for our understanding of the aggregation mechanisms of amyloid proteins *in vitro* and *in vivo*. However, amyloid oligomers have highly polymorphic, transitional, and aggregated structures, thus it is extremely difficult to design effective fluorescent probes (not limited to AIE probes) to recognize amyloids with different compositions, structures, and sizes *in vitro*, *ex vivo*, or *in vivo*. Ideally, the isolation of amyloid oligomers with well-defined sizes and structures is critical for identifying and understanding the role of AIE-based molecules in amyloid aggregation and toxicity. Also, the identified toxic amyloid oligomers, if any, could be used as specific biomarkers for the better design of AIE molecules and for better understanding both AIE mechanism and amyloid aggregation mechanism. Additional challenge is that different AIE–amyloid interactions are likely to modulate amyloid aggregation pathways in different manners towards different on-pathway or off-pathway binding species.

Most of the existing AIE probes are mostly limited to a single-target or a single-mode detection, leading to high failure rates of these amyloid probes in clinical trials.[39] More importantly, recent findings in amyloid cross-seeding (or "proteinopathies") show the prevalent co-existence and mixtures of different amyloid proteins in blood plasma and cerebrospinal fluids, in correlation with the co-occurrence of different amyloid diseases in the same individuals.[40] This fact indicates that single-target amyloid probes with single-mode detection would not be sufficient to detect different amyloid proteins that are pathologically linked to each other. From a broader viewpoint, considering that many amyloid proteins share similar structural, kinetic, and toxicity features, it is highly possible to develop some generic AIE-based molecules to recognize all/most of them for achieving the same/similar functions of sensing, monitoring, imaging, tracking, diagnosis, and even medical therapy. Thus, it remains a promising challenge to develop new multi-target/multi-mode AIE probes/sensors with improved sensitivity and selectivity for the detection of homo- and hetero-aggregates of different amyloid proteins. First, multimodal AIE probes allow integration of different molecular recognition mechanisms into a single molecule so as to synergistically promote their detection sensitivity and specificity. Second, multimodal AIE probes allow for the detection of different amyloid proteins and cross-amyloid aggregates. Third, multimodal AIE probes allow for validation of the results using orthogonal modalities. So, development of multimodal amyloid probes will offer critical insights into new fundamental understanding of amyloidosis and novel design principles for AIE probes/sensors.

With the recent and fast advance of data-driven artificial intelligence (AI), despite a relatively small dataset of AIE molecules, it is a still smart move to develop novel data/model-driven deep-learning algorithms for the rational design of new AIE molecules or repurposing of existing AIE molecules in an expedited way. AI models allow one to extract the structure–property features from even a small dataset of compounds, which would probably offer several structural templates for further design of new AIE molecules. The AI-driven design strategy would be able to greatly enlarge a pool of AIE molecules. Moreover, any successful or failed design can feedback to the AI models for data training and optimization in an iterative way, ultimately achieving highly efficient designs for AIE molecules. In parallel to AI modeling, AIE–amyloid interactions remain a key factor in understanding both AIE and amyloid aggregation mechanisms. Molecular simulations including quantum mechanics, molecular dynamics, and molecular docking are powerful tools to search and identify the binding modes (*e.g.*, binding affinity, sites, specificity) between AIE and amyloid aggregates at atomic levels. Computational mutagenesis can further confirm the key binding sequences, quaternary structures, and hotspot residues of amyloids as possible AIE targets. Further, more advanced hardware techniques (*e.g.*, GPU-based simulations) and algorithms (*e.g.*, graph theory) may allow one to map out the complex interaction patterns for a given AIE–amyloid system.

While AIE-based molecules hold substantial promise in the monitoring, diagnosis, and probable prevention of amyloid

2292 | *J. Mater. Chem. B*, 2022, **10**, 2280–2295

This journal is © The Royal Society of Chemistry 2022

proteins and their associated amyloid diseases, many challenges still remain and need to be addressed to achieve these goals. Among them, a more comprehensive understanding of both AIE and amyloid aggregation/toxicity mechanisms (*i.e.*, complex interplays between AIE molecules and amyloid proteins) is of the most paramount importance for the rational design of AIE molecules for amyloid aggregates. In addition, when applying AIE molecules to (pre)clinical applications for amyloid diseases, we anticipate that several potential issues of AIE molecules need to be addressed: (i) the poor solubility of AIE molecules makes them difficult to be dissolved in human body fluids (*e.g.*, blood, spinal fluid) for diagnostic purposes; (ii) the low BBB permeability of AIE molecules also leads to inefficient amyloid targeting/imaging through neuron cells, (iii) AIE molecules as common organic fluorescent molecules in the bloodstream may also result in three distinct issues of toxicity, immunogenicity, and rapid clearance by the mononuclear phagocyte system, and (iv) single AIE molecules usually cannot achieve the multifunction of biocompatibility, immunogenicity, BBB penetration, and cell/therapeutic targeting. Looking ahead, it is a great challenge but not an impossible one to overcome these limitations by developing new AIE molecules and AIE conjugates for organelle imaging, cancer biomarkers, cell targeting/tracking, and bacteria/pathogen imaging. We hope that this outlook may bring together researchers from various areas to explore many interesting aspects and bench-to-bedside applications of AIE-active molecules.

Conflicts of interest

There are no conflicts to declare.

Acknowledgements

References

1 J. Mei, Y. Huang and H. Tian, Progress and trends in AIE-based bioprobes: A brief overview., *ACS Appl. Mater. Interfaces*, 2018, **10**(15), 12217–12261.

2 J. Luo, Z. Xie, J. W. Lam, L. Cheng, H. Chen, C. Qiu, H. S. Kwok, X. Zhan, Y. Liu and D. Zhu, Aggregation-induced emission of 1-methyl-1,2,3,4,5-pentaphenylsilole, *Chem. Commun.*, 2001, 1740–1741.

3 J. Chen, C. C. Law, J. W. Lam, Y. Dong, S. M. Lo, I. D. Williams, D. Zhu and B. Z. Tang, Synthesis, light emission, nanoaggregation, and restricted intramolecular rotation of 1,1-substituted 2,3,4,5-tetraphenylsiloles, *Chem. Mater.*, 2003, **15**(7), 1535–1546.

4 Y. Hong, J. W. Lam and B. Z. Tang, Aggregation-induced emission: phenomenon, mechanism and applications, *Chem. Commun.*, 2009, 4332–4353.

5 R. Hu, S. Li, Y. Zeng, J. Chen, S. Wang, Y. Li and G. Yang, Understanding the aggregation induced emission enhancement for a compound with excited state intramolecular proton transfer character, *Phys. Chem. Chem. Phys.*, 2011, **13**(6), 2044–2051.

6 J. Guan, Q. Tu, L. Chen, M.-S. Yuan and J. Wang, A benzothiazole-rhodol based luminophor: ESIPT-induced AIE and an application for detecting Fe^{2+} ion, *Spectrochim. Acta, Part A*, 2019, **220**, 117114.

7 R. Long, C. Tang, J. Xu, T. Li, C. Tong, Y. Guo, S. Shi and D. Wang, Novel natural myricetin with AIE and ESIPT characteristics for selective detection and imaging of superoxide anions in vitro and in vivo., *Chem. Commun.*, 2019, **55**(73), 10912–10915.

8 Y. Wang, T. Liu, L. Bu, J. Li, C. Yang, X. Li, Y. Tao and W. Yang, Aqueous nanoaggregation-enhanced one-and two-photon fluorescence, crystalline J-aggregation-induced red shift, and amplified spontaneous emission of 9,10-bis(*p*-dimethylaminostyryl) anthracene, *J. Phys. Chem. C*, 2012, **116**(29), 15576–15583.

9 B.-K. An, S.-K. Kwon, S.-D. Jung and S. Y. Park, Enhanced emission and its switching in fluorescent organic nanoparticles., *J. Am. Chem. Soc.*, 2002, **124**(48), 14410–14415.

10 D. Kim, U. Lee, J. Bouffard and Y. Kim, Glycosaminoglycan-induced emissive J-aggregate formation in a meso-ester BODIPY dye, *Adv. Opt. Mater.*, 2020, **8**(14), 1902161.

11 G. Han, D. Kim, Y. Park, J. Bouffard and Y. Kim, Excimers beyond pyrene: A far-red optical proximity reporter and its application to the label-free detection of DNA., *Angew. Chem.*, 2015, **127**(13), 3984–3988.

12 A. V. Marsh, N. J. Cheetham, M. Little, M. Dyson, A. J. White, P. Beavis, C. N. Warriner, A. C. Swain, P. N. Stavrinou and M. Heeney, Carborane-induced excimer emission of severely twisted bis-*o*-carboranyl chrysene., *Angew. Chem.*, 2018, **130**(33), 10800–10805.

13 R. Hu, E. Lager, A. Aguilar-Aguilar, J. Liu, J. W. Lam, H. H. Sung, I. D. Williams, Y. Zhong, K. S. Wong and E. Pena-Cabrera, Twisted intramolecular charge transfer and aggregation-induced emission of BODIPY derivatives, *J. Phys. Chem. C*, 2009, **113**(36), 15845–15853.

14 E. Wang, J. W. Lam, R. Hu, C. Zhang, Y. S. Zhao and B. Z. Tang, Twisted intramolecular charge transfer, aggregation-induced emission, supramolecular self-assembly and the optical waveguide of barbituric acid-functionalized tetraphenylethene, *J. Mater. Chem. C*, 2014, **2**(10), 1801–1807.

15 J. D. Zhang, J. Mei, X. L. Hu, X. P. He and H. Tian, Ratiometric detection of β-amyloid and discrimination from lectins by a supramolecular AIE glyconanoparticle, *Small*, 2016, **12**(47), 6562–6567.

16 A. Aliyan, N. P. Cook and A. A. Martí, Interrogating amyloid aggregates using fluorescent probes, *Chem. Rev.*, 2019, **119**(23), 11819–11856.

17 A. Nabers, J. Ollesch, J. Schartner, C. Kötting, J. Genius, H. Hafermann, H. Klafki, K. Gerwert and J. Wiltfang,

This journal is © The Royal Society of Chemistry 2022

J. Mater. Chem. B, 2022, **10**, 2280–2295 | **2293**

Amyloid-β-secondary structure distribution in cerebrospinal fluid and blood measured by an immuno-infrared-sensor: A biomarker candidate for Alzheimer's disease., *Anal. Chem.*, 2016, **88**(5), 2755–2762.

18 W. Fu, C. Yan, Z. Guo, J. Zhang, H. Zhang, H. Tian and W.-H. Zhu, Rational design of near-infrared aggregation-induced-emission-active probes: in situ mapping of amyloid-β plaques with ultrasensitivity and high-fidelity, *J. Am. Chem. Soc.*, 2019, **141**(7), 3171–3177.

19 M. Gao and B. Z. Tang, Fluorescent sensors based on aggregation-induced emission: recent advances and perspectives, *ACS Sens.*, 2017, **2**(10), 1382–1399.

20 J. Shi, Y. Li, Q. Li and Z. Li, Enzyme-responsive bioprobes based on the mechanism of aggregation-induced emission, *ACS Appl. Mater. Interfaces*, 2017, **10**(15), 12278–12294.

21 J. Mei, Y. Huang and H. Tian, Progress and trends in AIE-based bioprobes: a brief overview, *ACS Appl. Mater. Interfaces*, 2017, **10**(15), 12217–12261.

22 C. Zhu, R. T. Kwok, J. W. Lam and B. Z. Tang, Aggregation-induced emission: A trailblazing journey to the field of biomedicine., *ACS Appl. Bio Mater.*, 2018, **1**(6), 1768–1786.

23 X. Cai and B. Liu, Aggregation-induced emission: Recent advances in materials and biomedical applications, *Angew. Chem.*, 2020, **132**(25), 9952–9970.

24 D. Mao and B. Liu, Biology-oriented design strategies of AIE theranostic probes, *Matter*, 2021, **4**(2), 350–376.

25 Y. Wang, J. Nie, W. Fang, L. Yang, Q. Hu, Z. Wang, J. Z. Sun and B. Z. Tang, Sugar-based aggregation-induced emission luminogens: Design, structures, and applications, *Chem. Rev.*, 2020, **120**(10), 4534–4577.

26 Y. Wang, Y. Qiu, A. Sun, Y. Xiong, H. Tan, Y. Shi, P. Yu, G. Roy, L. Zhang and J. Yan, Dual-functional AIE fluorescent probes for imaging β-amyloid plaques and lipid droplets, *Anal. Chim. Acta*, 2020, **1133**, 109–118.

27 J. Dai, X. Wu, S. Ding, X. Lou, F. Xia, S. Wang and Y. Hong, Aggregation-induced emission photosensitizers: from molecular design to photodynamic therapy: Miniperspective., *J. Med. Chem.*, 2020, **63**(5), 1996–2012.

28 R. Nelson and D. Eisenberg, Structural models of amyloid-like fibrils, *Adv. Protein Chem.*, 2006, **73**, 235–282.

29 M. Bucciantini, G. Calloni, F. Chiti, L. Formigli, D. Nosi, C. M. Dobson and M. Stefani, Prefibrillar amyloid protein aggregates share common features of cytotoxicity, *J. Biol. Chem.*, 2004, **279**(30), 31374–31382.

30 C. M. Dobson, Protein aggregation and its consequences for human disease., *Protein Pept. Lett.*, 2006, **13**(3), 219–227.

31 R. Kayed, E. Head, J. L. Thompson, T. M. McIntire, S. C. Milton, C. W. Cotman and C. G. Glabe, Common structure of soluble amyloid oligomers implies common mechanism of pathogenesis., *Science*, 2003, **300**(5618), 486–489.

32 C. W. T. Leung, F. Guo, Y. Hong, E. Zhao, R. T. K. Kwok, N. L. C. Leung, S. Chen, N. N. Vaikath, O. M. El-Agnaf and Y. Tang, Detection of oligomers and fibrils of α-synuclein by AIEgen with strong fluorescence., *Chem. Commun.*, 2015, **51**(10), 1866–1869.

33 M. Kumar, Y. Hong, D. C. Thorn, H. Ecroyd and J. A. Carver, Monitoring early-stage protein aggregation by an aggregation-induced emission fluorogen., *Anal. Chem.*, 2017, **89**(17), 9322–9329.

34 A. Das, A. Gupta, Y. Hong, J. A. Carver and S. Maiti, A spectroscopic marker for structural transitions associated with amyloid-β aggregation, *Biochemistry*, 2020, **59**(19), 1813–1822.

35 C. H. Wolstenholme, H. Hu, S. Ye, B. E. Funk, D. Jain, C.-H. Hsiung, G. Ning, Y. Liu, X. Li and X. Zhang, Aggfluor: fluorogenic toolbox enables direct visualization of the multi-step protein aggregation process in live cells, *J. Am. Chem. Soc.*, 2020, **142**(41), 17515–17523.

36 S. Ding, B. Yao, L. Schobben and Y. Hong, Barbituric acid based fluorogens: Synthesis, aggregation-induced emission, and protein fibril detection., *Molecules*, 2020, **25**(1), 32.

37 Y. Yang, S. Li, Q. Zhang, Y. Kuang, A. Qin, M. Gao, F. Li and B. Z. Tang, An AIE-active theranostic probe for light-up detection of Aβ aggregates and protection of neuronal cells, *J. Mater. Chem. B*, 2019, **7**(15), 2434–2441.

38 M. G. Iadanza, M. P. Jackson, E. W. Hewitt, N. A. Ranson and S. E. Radford, A new era for understanding amyloid structures and disease., *Nat. Rev. Mol. Cell Biol.*, 2018, **19**(12), 755–773.

39 Y. Zhang, B. Ren, D. Zhang, Y. Liu, M. Zhang, C. Zhao and J. Zheng, Design principles and fundamental understanding of biosensors for amyloid-β detection, *J. Mater. Chem. B*, 2020, **8**(29), 6179–6196.

40 B. Ren, Y. Zhang, M. Zhang, Y. Liu, D. Zhang, X. Gong, Z. Feng, J. Tang, Y. Chang and J. Zheng, Fundamentals of cross-seeding of amyloid proteins: an introduction, *J. Mater. Chem. B*, 2019, **7**(46), 7267–7282.

41 Y. Hong, L. Meng, S. Chen, C. W. T. Leung, L.-T. Da, M. Faisal, D.-A. Silva, J. Liu, J. W. Y. Lam and X. Huang, Monitoring and inhibition of insulin fibrillation by a small organic fluorogen with aggregation-induced emission characteristics, *J. Am. Chem. Soc.*, 2012, **134**(3), 1680–1689.

42 N. Pradhan, D. Jana, B. K. Ghorai and N. R. Jana, Detection and monitoring of amyloid fibrillation using a fluorescence "switch-on" probe, *ACS Appl. Mater. Interfaces*, 2015, **7**(46), 25813–25820.

43 C. Fan, Z.-Q. Chen, C. Li, Y.-L. Wang, Q. Yu and M.-Q. Zhu, Hydrophilic AIE-Active tetraarylethenes for fluorescence sensing and super-resolution imaging of amyloid fibrils from hen egg white lysozyme, *ACS Appl. Mater. Interfaces*, 2021, **13**(17), 19625–19632.

44 M. Z. Chen, N. S. Moily, J. L. Bridgford, R. J. Wood, M. Radwan, T. A. Smith, Z. Song, B. Z. Tang, L. Tilley and X. Xu, A thiol probe for measuring unfolded protein load and proteostasis in cells, *Nat. Commun.*, 2017, **8**(1), 1–11.

45 L. Jia, W. Wang, Y. Yan, R. Hu, J. Sang, W. Zhao, Y. Wang, W. Wei, W. Cui, G. Yang, F. Lu, J. Zheng and F. Liu, General aggregation-induced emission probes for amyloid inhibitors with dual inhibition capacity against amyloid β-protein and α-synuclein, *ACS Appl. Mater. Interfaces*, 2020, **12**(28), 31182–31194.

46 Y.-L. Wang, C. Fan, B. Xin, J.-P. Zhang, T. Luo, Z.-Q. Chen, Q.-Y. Zhou, Q. Yu, X.-N. Li, Z.-L. Huang, C. Li, M.-Q. Zhu and B. Z. Tang, AIE-based super-resolution imaging probes for β-amyloid plaques in mouse brains, *Mater. Chem. Front.*, 2018, **2**(8), 1554–1562.

47 C. Fan, Y.-L. Wang, P.-J. Zhao, H.-Q. Qu, Y.-X. Su, C. Li and M.-Q. Zhu, AIE-based dynamic *in situ* nanoscale visualization of amyloid fibrillation from hen egg white lysozyme, *Bioconjugate Chem.*, 2020, **31**(10), 2303–2311.

48 A. K. Mora, S. Murudkar, N. Shivran, S. Mula, S. Chattopadhyay and S. Nath, Monitoring the formation of insulin oligomers using a NIR emitting glucose-conjugated BODIPY dye, *Int. J. Biol. Macromol.*, 2021, **166**, 1121–1130.

49 N. R. Marzano, K. M. Wray, C. L. Johnston, B. P. Paudel, Y. Hong, A. van Oijen and H. Ecroyd, An α-cyanostilbene derivative for the enhanced detection and imaging of amyloid fibril aggregates, *ACS Chem. Neurosci.*, 2020, **11**(24), 4191–4202.

50 Y. Cui, C. Yuan, H. Tan, Z. Zhang, Y. Jia, N. Na and J. Ouyang, Plasmon-enhanced fluorescent sensor based on aggregation-induced emission for the study of protein conformational transformation, *Adv. Funct. Mater.*, 2019, **29**(10), 1807211.

51 Y. Jia, S. Guo, Q. Han, J. Zhu, X. Zhang, N. Na and J. Ouyang, Target-triggered and controlled release plasmon-enhanced fluorescent AIE probe for conformational monitoring of insulin fibrillation, *J. Mater. Chem. B*, 2021, **9**(25), 5128–5135.

52 Q. Huang, J. Xie, Y. Liu, A. Zhou and J. Li, Detecting the formation and transformation of oligomers during insulin fibrillation by a dendrimer conjugated with aggregation-induced emission molecule, *Bioconjugate Chem.*, 2017, **28**(4), 944–956.

53 N. Gour, V. Kshtriya, S. Gupta, B. Koshti, R. Singh, D. Patel and K. B. Joshi, Synthesis and aggregation studies of a pyridothiazole-based aiee probe and its application in sensing amyloid fibrillation, *ACS Appl. Bio Mater.*, 2019, **2**(10), 4442–4455.

54 A. Uddin, B. Roy, G. P. Jose, S. S. Hossain and P. Hazra, Sensing and modulation of amyloid fibrils by photoswitchable organic dots, *Nanoscale*, 2020, **12**(32), 16805–16818.

55 Z. Zhao, J. W. Lam and B. Z. Tang, Tetraphenylethene: a versatile AIE building block for the construction of efficient luminescent materials for organic light-emitting diodes., *J. Mater. Chem.*, 2012, **22**(45), 23726–23740.

56 W. Qin, J. Liu, S. Chen, J. W. Lam, M. Arseneault, Z. Yang, Q. Zhao, H. S. Kwok and B. Z. Tang, Crafting NPB with tetraphenylethene: A win–win strategy to create stable and efficient solid-state emitters with aggregation-induced emission feature, high hole-transporting property and efficient electroluminescence, *J. Mater. Chem. C*, 2014, **2**(19), 3756–3761.

57 L. Zong, Y. Xie, C. Wang, J.-R. Li, Q. Li and Z. Li, From ACQ to AIE: the suppression of the strong π–π interaction of naphthalene diimide derivatives through the adjustment of their flexible chains, *Chem. Commun.*, 2016, **52**(77), 11496–11499.

58 D. D. La, S. V. Bhosale, L. A. Jones and S. V. Bhosale, Tetraphenylethylene-based AIE-active probes for sensing applications, *ACS Appl. Mater. Interfaces*, 2017, **10**(15), 12189–12216.

59 M. Sakono and T. Zako, Amyloid oligomers: Formation and toxicity of Aβ oligomers. The, *FEBS J.*, 2010, **277**(6), 1348–1358.

60 F. Langer, Y. S. Eisele, S. K. Fritschi, M. Staufenbiel, L. C. Walker and M. Jucker, Soluble Aβ seeds are potent inducers of cerebral β-amyloid deposition., *J. Neurosci.*, 2011, **31**(41), 14488–14495.

61 B. Chandra, D. Bhowmik, B. K. Maity, K. R. Mote, D. Dhara, R. Venkatramani, S. Maiti and P. K. Madhu, Major reaction coordinates linking transient amyloid-β oligomers to fibrils measured at atomic level, *Biophys. J.*, 2017, **113**(4), 805–816.

62 M. Schledorn, B. H. Meier and A. Böckmann, Alternative salt bridge formation in Aβ—A hallmark of early-onset Alzheimer's disease?, *Front. Mol. Biosci.*, 2015, **2**, 14.

63 Y. Hong, J. W. Lam and B. Z. Tang, Aggregation-induced emission, *Chem. Soc. Rev.*, 2011, **40**(11), 5361–5388.

64 W. Yang, C. Liu, S. Lu, J. Du, Q. Gao, R. Zhang, Y. Liu and C. Yang, AIE-active smart cyanostyrene luminogens: Polymorphism-dependent multicolor mechanochromism, *J. Mater. Chem. C*, 2018, **6**(2), 290–298.

65 Z. Guo, A. Shao and W.-H. Zhu, Long wavelength AIEgen of quinoline-malononitrile, *J. Mater. Chem. C*, 2016, **4**(14), 2640–2646.

66 L. L. Marshall, S. E. Stimpson, R. Hyland, J. R. Coorssen and S. J. Myers, Increased lipid droplet accumulation associated with a peripheral sensory neuropathy, *J. Chem. Biol.*, 2014, **7**(2), 67–76.

67 C. Shi, Z. Guo, Y. Yan, S. Zhu, Y. Xie, Y. S. Zhao, W. Zhu and H. Tian, Self-assembly solid-state enhanced red emission of quinolinemalononitrile: Optical waveguides and stimuli response, *ACS Appl. Mater. Interfaces*, 2013, **5**(1), 192–198.

68 J. Zhao, Z. Chi, Z. Yang, Z. Mao, Y. Zhang, E. Ubba and Z. Chi, Recent progress in the mechanofluorochromism of distyrylanthracene derivatives with aggregation-induced emission., *Mater. Chem. Front.*, 2018, **2**(9), 1595–1608.

69 J. He, B. Xu, F. Chen, H. Xia, K. Li, L. Ye and W. Tian, Aggregation-induced emission in the crystals of 9,10-distyrylanthracene derivatives: The essential role of restricted intramolecular torsion, *J. Phys. Chem. C*, 2009, **113**(22), 9892–9899.

70 B. Xu, J. Zhang, S. Ma, J. Chen, Y. Dong and W. Tian, 9,10-Distyrylanthracene derivatives: Aggregation induced emission, mechanism and their applications, *Prog. Chem.*, 2013, **25**(7), 1079.

This journal is © The Royal Society of Chemistry 2022

J. Mater. Chem. B, 2022, **10**, 2280–2295 | **2295**